J Mater Sci (2011) 46:6571–6580
DOI 10.1007/s10853-011-5604-7

Enhancement of the thermal conductivity of aluminum oxide–epoxy terminated poly(dimethyl siloxane) with a metal oxide containing polysiloxane

Hyungu Im · Jooheon Kim

Received: 1 February 2011 / Accepted: 2 May 2011 / Published online: 13 May 2011
© Springer Science+Business Media, LLC 2011

Abstract Aluminum oxide containing poly(dimethylmethylvinyl)siloxane (PMDMS:Al_2O_3) was synthesized and blended with epoxy-terminated dimethylsiloxane (ETDS) to fabricate a thermally conducting composite. PMDMS:Al_2O_3 was added to provide interfacial interactions between the Al_2O_3 and polymer matrix. The PMDMS:Al_2O_3 containing composites revealed more enhanced thermal conduction properties because of the strengthened interfacial bonding at a fixed filler concentration. The conductivity as a function of the filler concentration was correlated with Agari's models. Based on the coefficient obtained from Agari's model, PMDMS:Al_2O_3 affected the formation of the conducting path in the composite. The results indicated that the presence of PMDMS:Al_2O_3 would help to establish a conducting path compared to compounds without it. All composites showed a decrease in thermal conductivity with increasing operating temperature. As expected, the PMDMS:Al_2O_3 containing composite (P-ETDS/Al_2O_3) showed more enhanced thermal conductivity than those without, regardless of the operating temperature.

Introduction

The progress for miniaturizing electronic device components has aggravated the problems associated with heat dissipation in the electronics industry and has produced a need for improved thermal interface materials (TIM) in modern chip packaging [1–3]. It is well known that the reliability of an electronic device is exponentially dependent on the operating temperature of the junction, whereby a small difference in the operating temperature (on the order of 10–15 °C) can result in a twofold reduction in the lifespan of a device [4]. Therefore, it is essentially crucial for the heat generated from the device to be dissipated as quickly and as effectively as possible to maintain the operating temperature of the device at a desired level [5, 6].

Traditionally, thermal issues in encapsulated devices have been addressed by the use of embedded heat sinks, which are often susceptible to thermal cracking and have limited utility in thinner packages [7]. Under this circumstance, polymers filled with thermally conductive fillers are emerging as a cost effective way to cope with thermal management issues [8].

Many studies have been performed to fabricate a thermally conductive composite as TIM. The literature concerning thermally conductive plastic composites is particularly focused on the use of different electrical insulative fillers, such as boron nitride (BN), aluminum nitride (AlN), and alumina oxide (Al_2O_3) [9–16]. Shi et al. [9] reported enhanced thermal conductivity (from 0.2 to 4.5 W/m K) of an epoxy composite filled with 3D brush-like AlN nanowhiskers, which was 2.3 times greater than that of a composite filled with the same content of commercial AlN equiaxed particles. However, these methods are not broadly adopted because the synthesis method of 3D brush-like particles was extremely complicated and not yet commercially available. Lee et al. reported the effect of the coupler content and temperature of thermal treatment on the thermal conductivity of the EVA–ZnO composites. They stated that the surface-treating ZnO filler with the valid modifying agents can improve the compatibility of the ZnO filler with the EVA matrix, and enhance the thermal conductivity of the EVA–ZnO composites on account of the decrease in interfacial phonon scattering

H. Im · J. Kim (✉)
School of Chemical Engineering & Material Science, Chung-Ang University, Seoul 156-756, Korea
e-mail: jooheonkim@cau.ac.kr

[13]. Lee et al. also studied well-dispersed AlN composites containing pre-treated filler and epoxy resin with low viscosity. They reported a 15 times greater thermal conductivity for the polymer matrix with a dispersant chemistry at high loading filler contents (close to 60 vol%) [14]. However, high filler loading could provide application restrictions because of its reduced workability and high production cost. Significant effort has been expelled to improve the thermal conductivities of composites for heat-dissipating applications [17–22].

As previously mentioned, most reported studies have focused on the particle treatment or modification of the process to promote the formation of a more effective percolating network of particles in the matrix.

The previous study indicated that well-dispersed conditions would enable the establishment of a conductive path, which would lead to a higher conductivity when the composite was near the percolation threshold [23]. Therefore, the most important factor for enhancing thermal conduction properties is the establishment of well-dispersed conducting particles.

Various TIMs are now available, such as elastomeric thermal pads and thermal greases [24]. As a matrix, polydimethylsiloxane (PDMS)-based materials are the most frequently adopted TIM matrices due to their unique properties, including a wide range of service temperatures, high flexibility, chemical resistance, and good electrical insulating properties [4, 24–28]. Goh and co-workers [4] showed a two-fold enhancement of thermal conductivity for PDMS filled with 10 vol% ZnO particles. Similarly, Wang and Xie [26] explored the heat-conductive silicone rubber filled with hybrid Al_2O_3 and AlN particles, and Zhou et al. [27] also investigated the Al_2O_3-reinforced heat-conductive composite silicone rubber.

In this study, a polymer matrix, dimethyl siloxane-based epoxy, was employed to fabricate a thermally conductive composite due to good flexibility and excellent electrical insulating properties [28]. Al_2O_3 was adopted as a thermally conductive and electrical insulating filler. To increase interfacial interactions, which is expected to provide good dispersion, synthesized Al_2O_3 containing modified polysiloxane prepared based on our previous study [29] was employed. In addition, the effect of metal oxide containing modified polysiloxane was investigated through the various thermal conductivity prediction models.

Experimental

Materials

The epoxy-terminated dimethylsiloxane (ETDS) was obtained from Shin-Etsu silicons (KF-105, equivalent weight (E.E.W) = 490 g/eq, density = 0.99 g/cm^3). 4,4′-Diaminodiphenylmethane (DDM), prepared by TCI Korea, was used as a curing agent without further purification. To prepare poly(dimethyl-methylvinyl)siloxane (PMDMS) as an interfacial interaction provider, octamethylcyclotetrasiloxane (D_4), 1,3,5,7-tetramethylcyclotetrasiloxane ($D_4^{Me,H}$), 1,3,5,7-tetravinyl-1,3,5,7-tetramethylcyclotetrasiloxane ($D_4^{Vi,Me}$), and 1,1,3,3-tetramethylsiloxane were purchased from Aldrich Chemical Co., Inc. (Milwaukee, WI) and were used after distillation under reduced pressure. As a catalyst, tetramethylammonium siloxaneolate (TMAS) was obtained through dehydration after a reaction between D_4 and tetramethylammonium hydroxide (Aldrich, 25 wt% in water). Both *N*,*N* dimethylacrylamide (DMAA) was supplied by Sigma Chemical Co. (St. Louis, MO). Aluminum oxide monodispersed spheres with diameters of approximately 5 nm and 10 μm were used as the filler and were supplied by Aldrich Chemical Co., Inc. (Milwaukee, WI).

Synthesis of ETDS–DDM

The ETDS oligomer was introduced to fabricate the matrix. Based on our previous study, the weight ratio of the epoxy to the curing agent was determined to provide efficient flexibility of the matrix [28]. In this study, the equivalent weight ratio of ETDS and DDM was 1:2. 1.9 g of DDM was placed in a four-neck round flask equipped with a reflux condenser and preheated to 363 K. 9.5 g of the ETDS resin was added and heated in an oil bath at 363 K for 1 h in N_2 atmosphere. The bubbles in the mixture were removed by placing the mixture in a vacuum oven for 30 min at room temperature. The mixture was then placed in an oil bath at 323 K for 10 min in N_2 atmosphere. The final degassing was performed in a vacuum oven for 1 h at room temperature to remove the air bubbles. The chemical structures of ETDS–DDM are illustrated in the Fig. 1.

Synthesis of Al_2O_3 containing PMDMS

The modified poly(methyl-dimethylmethylvinyl)siloxane (PMDMS) was synthesized using a previously described equilibrium polymerization method [29–31]. This method involved reactions between 2.9 g of D_4, 7.2 g of $D_4^{Me,H}$, and 3.4 g of $D_4^{Vi,Me}$ in the presence of TMAS catalyst with 1:3:1 molar ratio, respectively. The reactions are shown in Fig. 2. Each PMDMS sample was prepared by first heating the mixture of monomers in a three-neck flask under a stream of nitrogen and then adding 0.2 wt% of TMAS catalyst to the mixture. The reaction was conducted at 80 °C for 48 h; then, the temperature was raised to 150 °C for 1 h to decompose the catalyst. The reaction rates of cyclosiloxane monomers to synthesize PMDMS were dependent on the acidity of each monomer, especially for the ring-opening

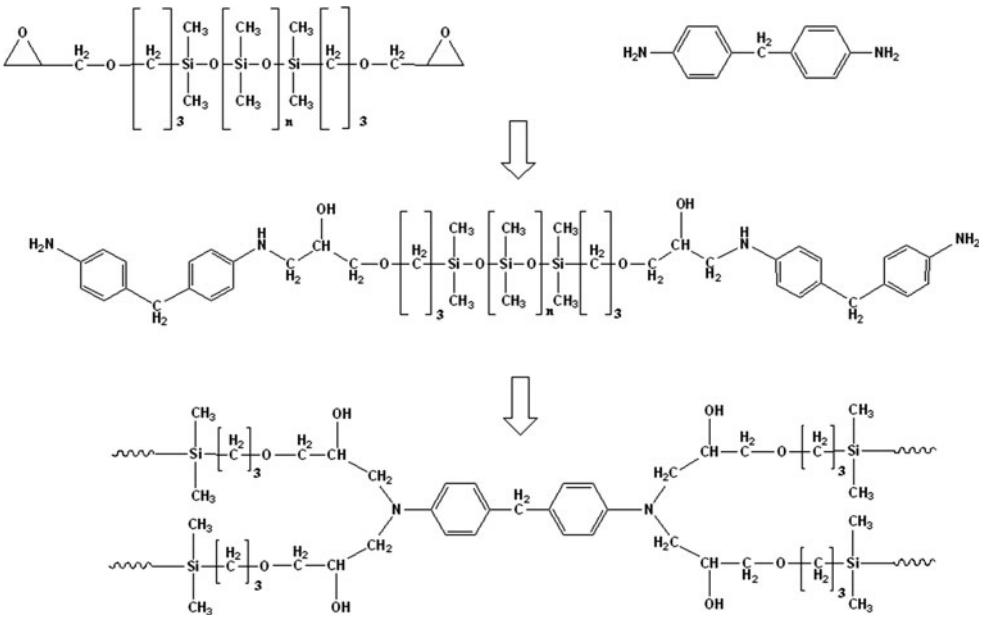

Fig. 1 Illustration of the cure system for ETDS with 4,4′-DDM

reactions. The weak base, TMAS, causes the ring-opening of $D_4^{Me,H}$, which has a higher acidity than either D_4 or $D_4^{Me,Vi}$. An open-ring $D_4^{Me,H}$ formed a methyl-siloxane block unit in the first step of the polymerization process. Subsequently, D_4 and $D_4^{Me,Vi}$ blocks were formed [26, 27]. The synthesized PMDMS containing Al_2O_3 (PMDMS: Al_2O_3) materials were analyzed through the same method used in our previously reported study [29]. Note that the vinyl group containing siloxane monomer which can be cured with Si–H in tails of chain was employed. These vinyl groups are reacted with Si–H in the presence of Pt catalyst, then it can easily form the cross-linked network.

After cooling, the mixture was subjected to vacuum stripping at room temperature for 1 h to remove residual monomers. The synthesized PMDMS reacted with *N*,*N* DMAA which have a molar ratio equal to mole fraction on $D_4^{Me,H}$ in PMDMS at 90 °C in the presence of the Pt catalyst (0.01 wt%) for 4 h. Then, excess aluminum oxide was added to the product, following stirring at 1500 rpm for 24 h to achieve coordination in the polymer chain. The grafted DMMA on the $D_4^{Me,H}$ block could be coordinated with the metal oxide because of its strong electronegativity balance [31].

Sample preparation

The Al_2O_3 particles with an average size of 10 μm were used in the preparation of the composites. The ETDS-based composites were prepared by mixing the Al_2O_3 particles with 10 wt% PMDMS:Al_2O_3 and zirconium beads to form well-dispersed Al_2O_3 particles. After mixing, the composites were casted onto a Teflon pan and were cured for 2 h at 180 °C.

Characterization

To verify the synthesis of polysiloxane, Fourier transform infrared (FT-IR) measurements were performed in the 3,200–600 cm^{-1} region using a horizontal attenuated total reflection (ATR) accessory and zinc selenate crystals. ^1H NMR (300 MHz, Gemini 2000, Varian) was also used to confirm each block ratio of the synthesized polysiloxane. Scanning electron microscopy (SEM, S-4300SE, Hitachi) was employed to investigate the dispersity of the filler in the ETDS composites. The thermal diffusivity of each sample was measured using a transient method, very similar to that used in laser-flash experiments. In this procedure, a temperature signal was transferred to the upper side of the sample and was measured using a thermocouple. This transferred signal initiated a thermal equilibration process in the specimen, which was recorded using a difference thermocouple at the rear surface and was used to evaluate the thermal diffusivity. The thermal conductivity was calculated using the following equation

$$k = \alpha \times \rho \times C_p \quad (1)$$

where k, α, ρ, and C_p represent the thermal conductivity (W/m K), thermal diffusivity (mm^2/s), density (g/cm^3), and specific heat capacity (J/kg K), respectively [32, 33].

Results and discussion

The FT-IR and ^1H-NMR were used to characterize the modified polysiloxane. The broad absorption bands in Fig. 3 are associated with the stretching band (1000–1250 cm^{-1}) of

Fig. 2 Synthesis of PMDMS

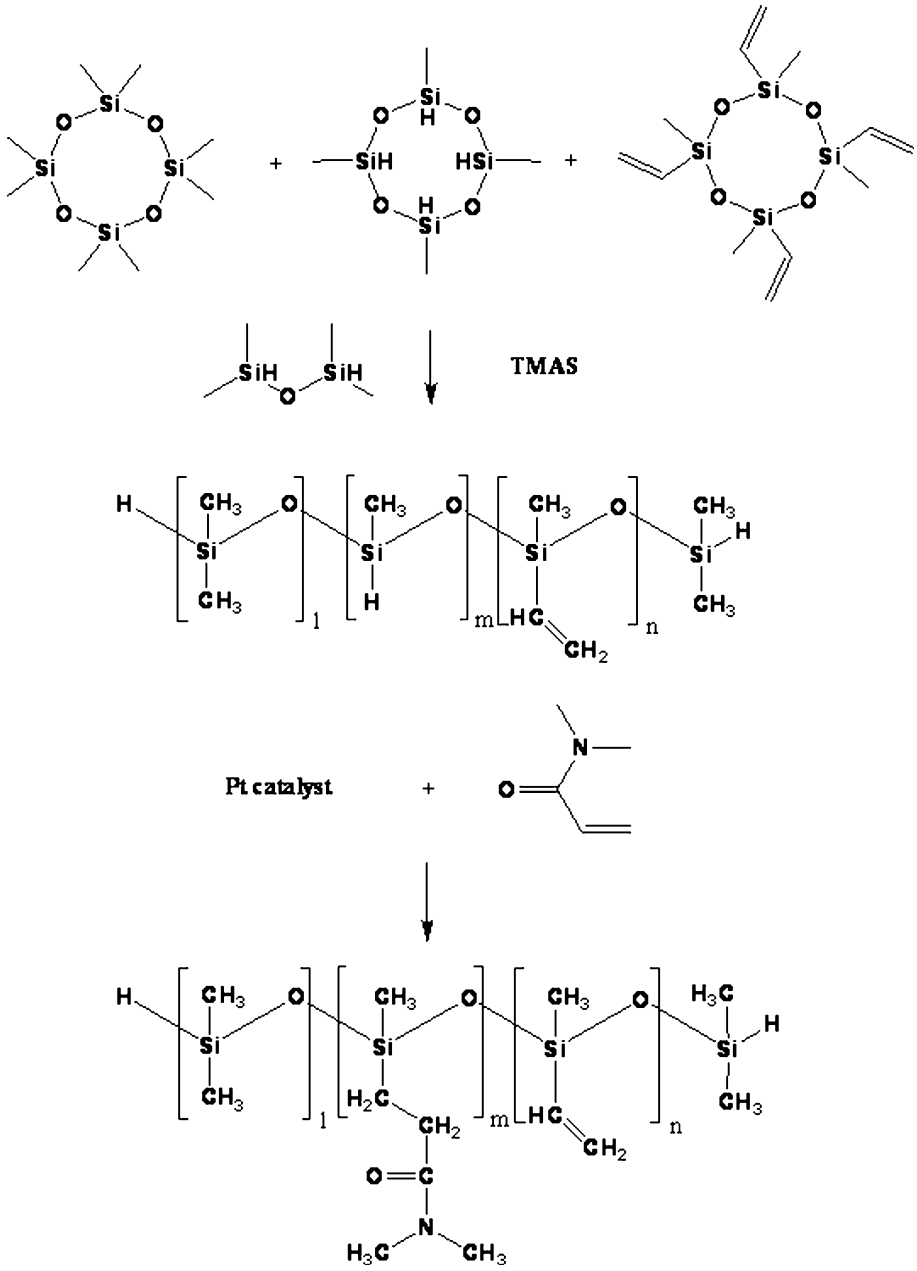

Si–O–Si. Smaller absorption bands, which can be attributed to the terminal vinyl groups, were clearly observed at 3079 cm^{-1} (=CH stretching), 1642 cm^{-1} (C=C stretching), and 910 cm^{-1} (=CH_2 out-of-plane deformation). Absorption bands due to Si–H and Si–CH_3 were observed at 2150 and 1250 cm^{-1}, respectively. Figure 3b shows the FT-IR spectra of PMDMS–DMA. As shown in Fig. 2, DMAA was grafted on the Si–H block by the siloxane-vinyl addition reaction. The grafting of DMAA was also confirmed by characteristic absorption bands at 1628 and 1451 cm^{-1}, which were assigned to the amide carbonyl (–C=O) and C–N stretching vibrations of the tertiary amide of DMAA. The above FT-IR data demonstrates that the DMAA had been attached successfully during synthesis. In addition, the weakening of the absorption band at 2150 cm^{-1} (Si–H absorption) in the FT-IR spectrum of PMDMS provided further evidence of the successful addition of DMAA to the PMDMS.

The block ratio of synthesized PMDMS was determined by the integration value of the ^{1}H NMR spectra, as shown in Fig. 4. Peaks for Si–H and Si–CH=CH_2 at 4.8 and 6.044–5.988 ppm, respectively, as shown in Fig. 4. In this figure, the integration value (IV*) divided by the number of protons in each group, i.e., 1 and 3, was 10 and 4.5, respectively. Consequently, the block ratio of $D_4^{Me,H}$ to $D_4^{Me,Vi}$ in the synthesized PMDMS was 2.22:1.

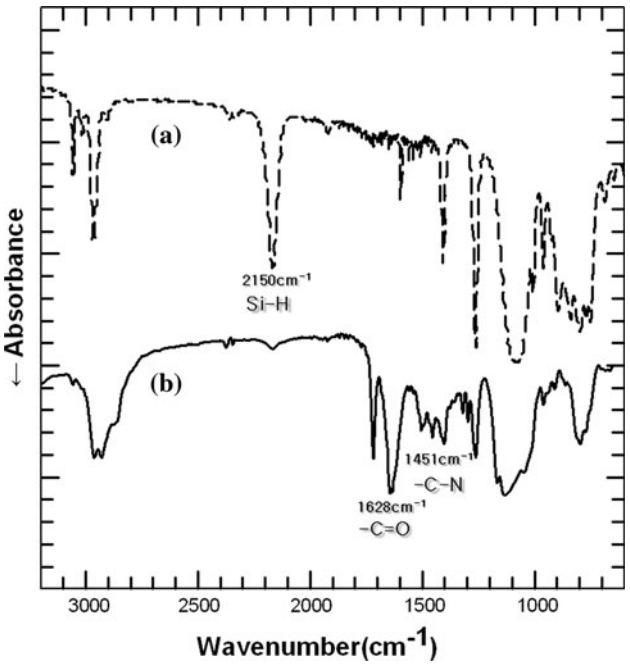

Fig. 3 FT-IR spectra of (*a*) synthesized PMDMS and (*b*) modified PMDMS:DMAA

The effect of PMDMS:Al_2O_3 materials on the dispersity of micro Al_2O_3 particles in the ETDS matrix was investigated using SEM analysis and are shown in Fig. 5. As shown in Fig. 5, the ETDS/Al_2O_3 composite without PMDMS:Al_2O_3 (ETDS/Al_2O_3) showed more aggregated Al_2O_3 particles in the composite matrix, and most of the aggregated particles were irregularly located on the surface. In addition, separated pores in the polymer matrix were observed due to the absence of interfacial interactions between the polymer matrix and the Al_2O_3 particles.

However, dispersion of Al_2O_3 particles in the ETDS matrix containing PMDMS:Al_2O_3 (P-ETDS/Al_2O_3) was much better than in that without, and a less porous structure was formed on the surface compared to that of PMDMS:Al_2O_3, as shown Fig. 5b. The differences between the cross-sectional surface morphologies of the composites can be correlated to the existence of Al_2O_3 coordinated in PMDMS.

The dimethylsiloxane block in the PMDMS can provide miscibility with the dimethylsiloxane unit of the ETDS matrix because of its similar chain structure [34, 35]. The miscibility of a PDMS-based polymer blend was investigated in a previous study. Barrie and Munday [34] reported the phase morphologies of blends composed of various polystyrene-PDMS copolymers, such as PS-g-PDMS and PS-b-PDMS. The results indicated that the PDMS block units of the blends composed of different co-polymers exhibited a continuous miscible phase and a dispersed PS domain structure in the co-polymer. Bajaj and Varshney [35] also reported that the tensile strength of the crosslinked PDMS increased by blending with PDMS-b-PS due to the partial miscibility between PDMS and the PDMS block co-polymer.

As indicated in the previous studies, dimethylsiloxane in the PMDMS can provide compatibility with dimethylsiloxane in the ETDS, and the dimethylsiloxane block in the PMDMS can be homogeneously dispersed in the ETDS matrix.

However, because other blocks formed from the D_4 coordinated in the Al_2O_3 and $D_4^{Vi,Me}$ were not compatible with the dimethylsiloxane block [36]. These blocks have to exist at the interface between Al_2O_3 and the ETDS matrix. The miscible phase and interfacial bonding between ETDS and Al_2O_3 are illustrated in Fig. 6. A phase-separated block containing Al_2O_3 easily aggregated with micro Al_2O_3

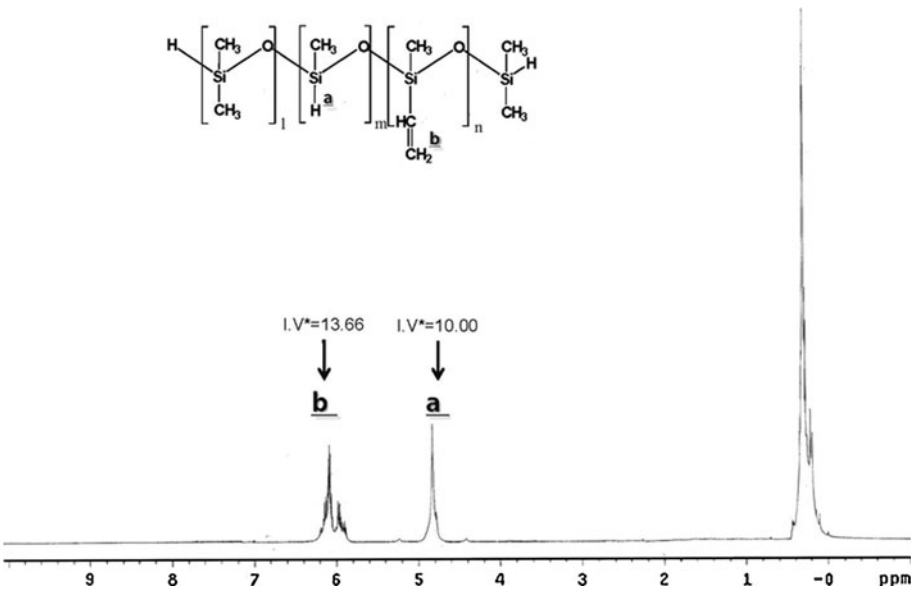

Fig. 4 ^1H NMR spectra of synthesized polysiloxane

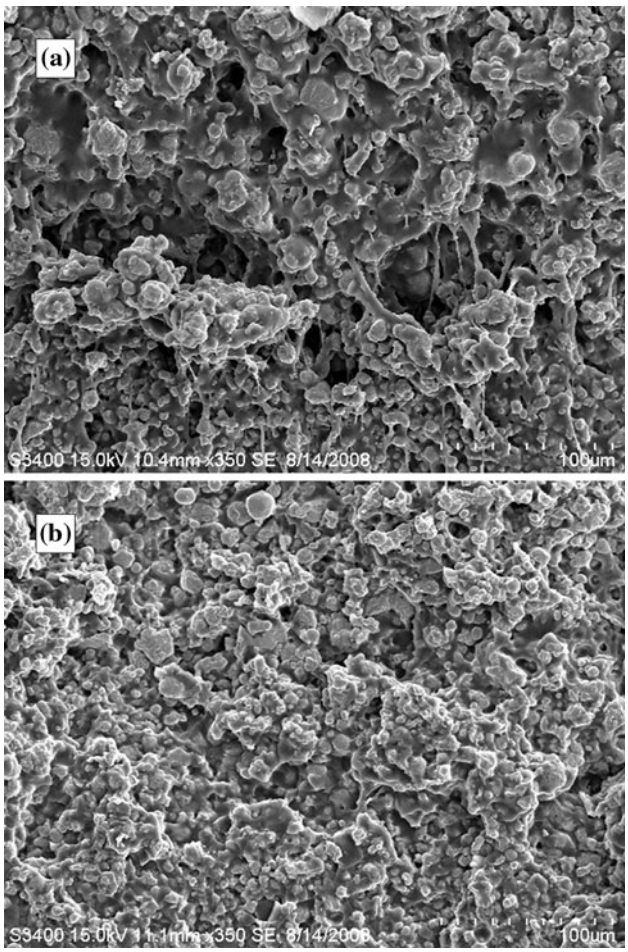

Fig. 5 SEM images of **a** ETDS/Al_2O_3 and **b** ETDS/PMDMS:Al_2O_3/Al_2O_3 composites

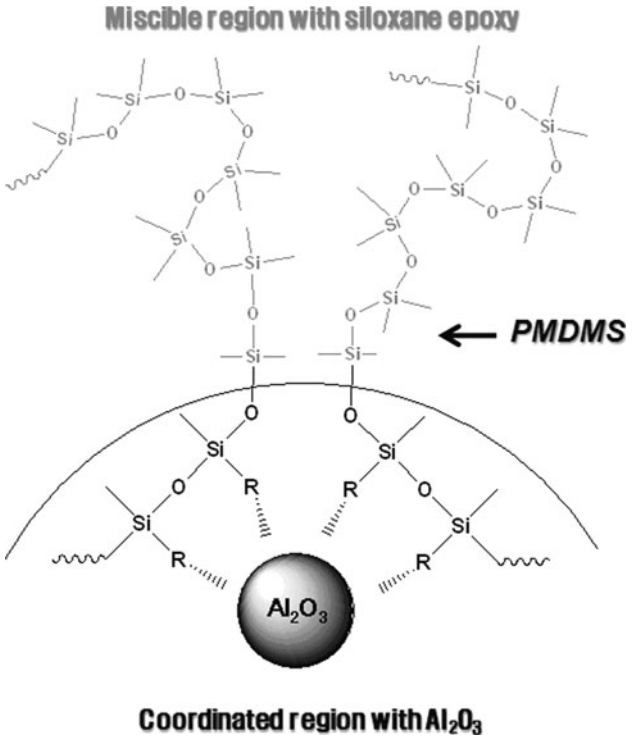

Fig. 6 Schematic diagram of PMDMS:Al_2O_3 role in the ETDS/PMDMS:Al_2O_3/Al_2O_3 composite

particles, and the aggregation between the Al_2O_3 particles and Al_2O_3 in the PMDMS improved interfacial bonding strength. In addition, the interactions of Al_2O_3 in PMDMS with micro Al_2O_3 may disturb the aggregation of microparticles in the polymer matrix when composites are fabricated using the curing method. Therefore, the addition of metal oxide containing PMDMS in the ETDS composite improved the particle dispersion caused by enhanced interfacial interaction strength.

The effect of PMDMS:Al_2O_3 content on its thermal conductivity was investigated with several fixed micro Al_2O_3 concentration and results are showed in the Fig. 7. As expected it, the addition of PMDMS:Al_2O_3 to the EDTS/Al_2O_3 provide the enhancement of thermal conductivity as a function of PMDMS:Al_2O_3 loading. Therefore, all of investigations in this study were used with a fixed concentration of PMDMS:Al_2O_3 which is 10 wt%.

The experimental dependences of thermal diffusivity and conductivity on filler volume content for the composite are shown in Fig. 8. The thermal conductivities of both composites increased with filler loading, whereby, at a fixed filler loading, the P-ETDS/Al_2O_3 composite showed higher thermal diffusivity and conductivity values compared to those without.

The higher thermal conductivity of the P-ETDS/Al_2O_3 was possibly due to its internal structure. The P-ETDS/Al_2O_3 can provide a more enhanced interfacial interaction between particles and ETDS caused by the coordinated Al_2O_3 in the PMDMS. With the addition of PMDMS:Al_2O_3 as a composite additive, regular particle distribution and a less porous structure allowed for an easier thermal diffusion in the polymer network compared to that without composite, as reported in Fig. 5. In this study, additional analytical analysis that provided clear evidence of the dispersity difference between these materials was employed.

Many theoretical models have been issued to explain the thermal conductivities of two-phased composites [37–46]. The Maxwell-Euken's model treats the thermal conductivities of composites consisting of homogeneously mixed and noninteracting spherical fillers in a homogenous matrix using the following equation [37, 38]:

$$\frac{k_c}{k_m} = \frac{k_f + 2k_m - 2\Phi_f(k_f - k_m)}{k_f + 2k_m + \Phi_f(k_f - k_m)}, \quad (2)$$

where k_c is the thermal conductivity of the composite, k_m is the thermal conductivity of the matrix, k_f is the thermal conductivity of the filler, and Φ_f is the volume percentage of the filler. This model fit well in a low solid loading

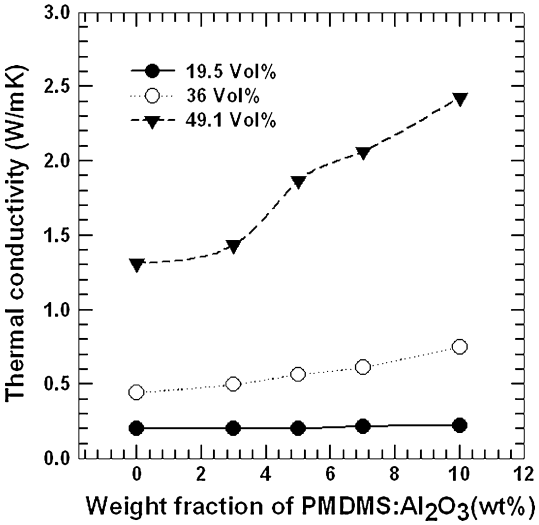

Fig. 7 The effect of PMDMS:Al_2O_3 contents on the thermal conductivity at fixed Al_2O_3 contents

where the particles were not touching. In the high solids loading range ($\Phi_f > 50$ vol%), a large deviation from the experimental value occurred because this model did not consider the particle packing factor or the interactions between the polymer matrix and particles [38].

Another useful theoretical model for high filler-loaded composites was first suggested by Meredith and Tobias with reasonable success [39]. Their equation for relative thermal conductivity was

$$\frac{k_c}{k_m} = \frac{(1+\Phi_f)(2+\Phi_f)}{(1-\Phi_f)(2-\Phi_f)}. \quad (3)$$

Another important model is that of Bruggeman [40], which considers the interactions between particles, but which is only a good prediction for volume fractions in up to 20% of the discrete phase [41]. The equation for this model is as follows:

$$1-\Phi_f = \frac{k_f - k_c}{k_f - k_m}\left(\frac{k_m}{k_c}\right)^{1/3}. \quad (4)$$

However, these models have not always been well correlated to the experimental results. The heat conduction model was considered, as it has various factors that can influence conducting behaviors, such as solids loading, particle size or shape, and homogeneity of the dispersed phase in the matrix [14].

Based on the factors that can affect the thermal conductivity, Ramajo et al. proposed a numerical model using the finite element method (FEM) with several different packing protocols to achieve reasonable thermal and electrical properties at high filler contents. They regarded the three possible packing protocols and calculated each numerical value expected by computer modeling. In addition, they showed more enhanced accuracy of the assumed

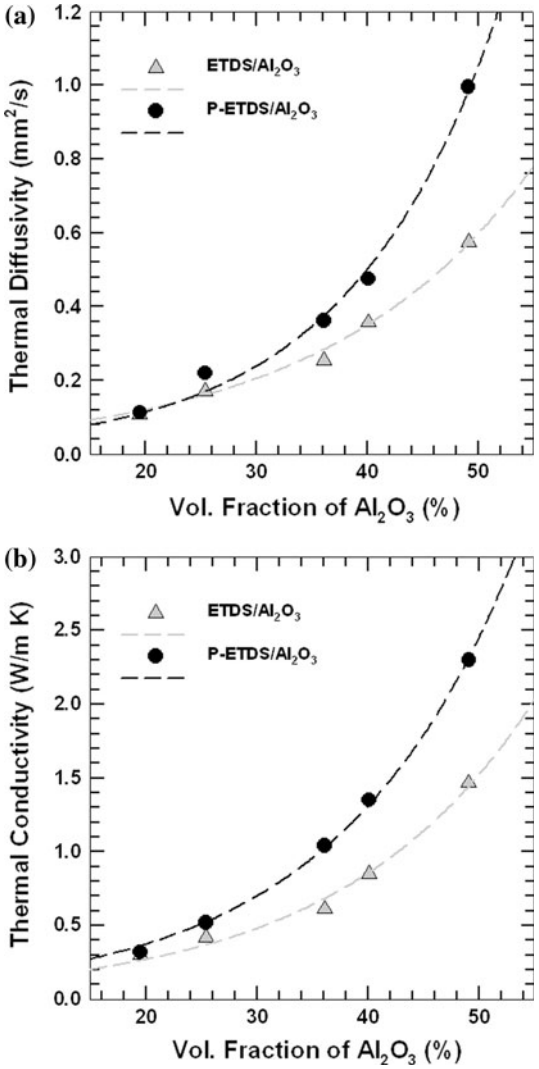

Fig. 8 Thermal conductive properties of composites as a function of the filler content: **a** thermal diffusivity and **b** thermal conductivity

packing protocol than the other empirical models [42]. Nevertheless, despite its accuracy at high filler content, it is not acceptable in terms of the objectives of this study because the analytical derived criteria that can indicate the formation of a thermal conductive path is necessary to confirm the effect of PMDMS materials based on their thermal conductive behavior.

Agari and Uno [43–46] modified the Maxwell model assuming that, with a certain probability P, the filler particles form conductivity paths in the polymer matrix. According to this theory, the thermal conductivity coefficient is calculated through the following equation

$$k_c = k_m \frac{k_f + 2k_m + 2(1-P)(k_f - k_m)}{k_f + 2k_m - P(k_f - k_m)} + \Phi_f P c^2 k_f, \quad (5)$$

where c^2 is the cross-sectional area of the conducting path, $P = (\Phi_f)^{(\Phi_f)^{-2/3}}$ and $\Phi_f = 3c^2 - 2c^3$ [43, 44]. In refs [43, 46],

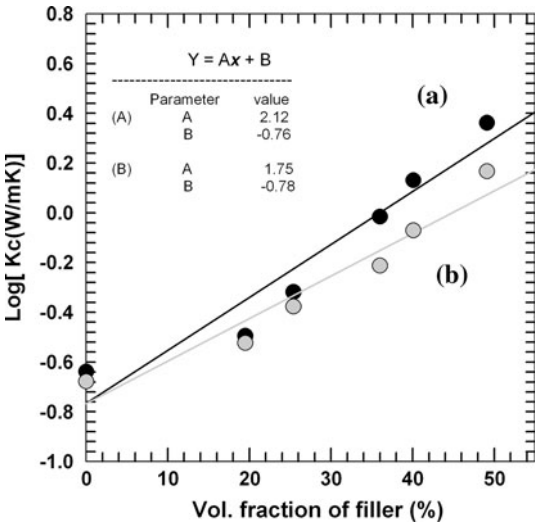

Fig. 9 Logarithm of thermal conductivity of Al_2O_3-filled composite linearly fit by the Agari and Uno models

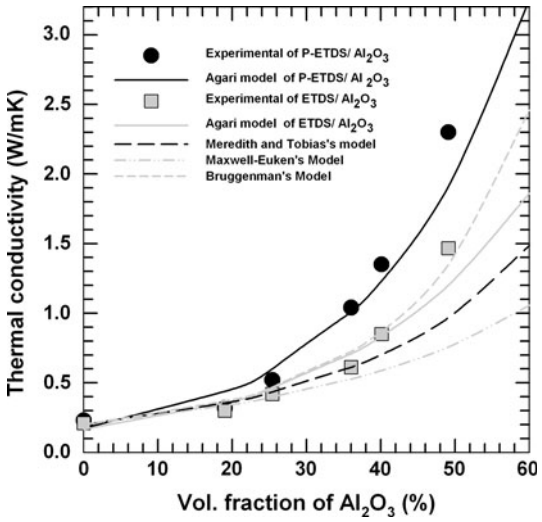

Fig. 10 Comparison of the measured thermal conductivities of Al_2O_3-filled composites with calculated thermal conductivities using various theoretical models

an alternative model was proposed for the estimation of the thermal conductivity of a blend containing more than two-phases, the equation of which is

$$\log k_c = \Phi_f[P^* - \log(C_1 k_m)] + \log(C_1 k_m), \quad (6)$$

where $P^* = X_2C_2\log k_f + X_3C_3\log k_3 + \ldots$; C_i is the factor accounting for the formation of the conducting paths in a matrix, and X_i is the ratio between the filler particles in the blend. In the case of single particles, X_1 is equal to 1 and the other coefficients are neglected.

This model's resulting equation is

$$\begin{aligned}\log k_c &= \Phi_f C_2 \log k_f + (1 - \Phi_f)\log(C_1 k_m) \\ &= (C_2 \log k_f - \log C_1 k_m)\Phi_f + \log(C_1 k_m). \end{aligned} \quad (7)$$

In order to obtain C_1 and C_2, the plot of log k_c versus Φ_f was obtained using data from Fig. 9. The slopes $(C_2\log k_f - \log C_1 k_m)$ of PMDMS:Al_2O_3 with and without composite were 2.12 and 1.75, respectively. In addition, the intercepts $[\log(C_1 k_m)]$ of the samples were -0.76 and -0.78, respectively.

The plot of the expected thermal conductivities of these materials using the Agari model was obtained after substituting the slope and intercept into Eq. 7, with the resulting equation being reported in Table 1.

Table 1 Thermal conductive characteristic equation and coefficients of composites according to Agari and Uno model

	In the presence of PMDMS:Al_2O_3	In the absence of PMDMS:Al_2O_3
Eq.	$k_c = 10^{(2.12\Phi_f - 0.76)}$	$k_c = 10^{(1.75\Phi_f - 0.78)}$
C_1	0.76	0.75
C_2	0.90	0.61

The expected thermal conductivities of several models described in this study are plotted in Fig. 10. Because Maxwell's model did not consider the particle's contact inside the polymer matrix, it predicted the lowest thermal conductivity. Meredith's model was also insufficient for describing the thermal conductivity in this study. Bruggeman's model was well correlated with the composite ETDS/Al_2O_3; however, the predicted value of Bruggeman's model showed a large deviation for the P-ETDS/Al_2O_3. Agari's model yielded better predictions than did the other models because of the two adjustable constants, C_1 and C_2, which were obtained from experimental results.

According to Agari models, C_1 is a factor relating to the effect of the filler on the secondary structure of the polymer, and C_2 is a factor relating to the formed conductive chain of the filler [45]. C_1 and C_2 should be between 0 and 1, and the closer the C_2 values are to 1, the more easily conductive chains are formed in the composite [43, 45, 46]. The calculated C_1 and C_2 values of the composite from Eq. 7 are listed in Table 1. The addition of PMDMS:Al_2O_3 into the ETDS composite affects the C_2 value more strongly than do the C_1 values. As reported in Table 1, C_1 was not dependent on the addition of PMDMS:Al_2O_3. Nevertheless, the C_2 value for the composite containing PMDMS:Al_2O_3 showed a value closer to 1 than those without. This indicates that the addition of the PMDMS:Al_2O_3 into ETDS did not affect the secondary structure of the polymer matrix but formed the conducting path. The improved filler dispersion and less porous structure in the composite was a result of the PMDMS:Al_2O_3, which enhanced the interfacial interaction strength between the polymer matrix and the aluminum oxide particles.

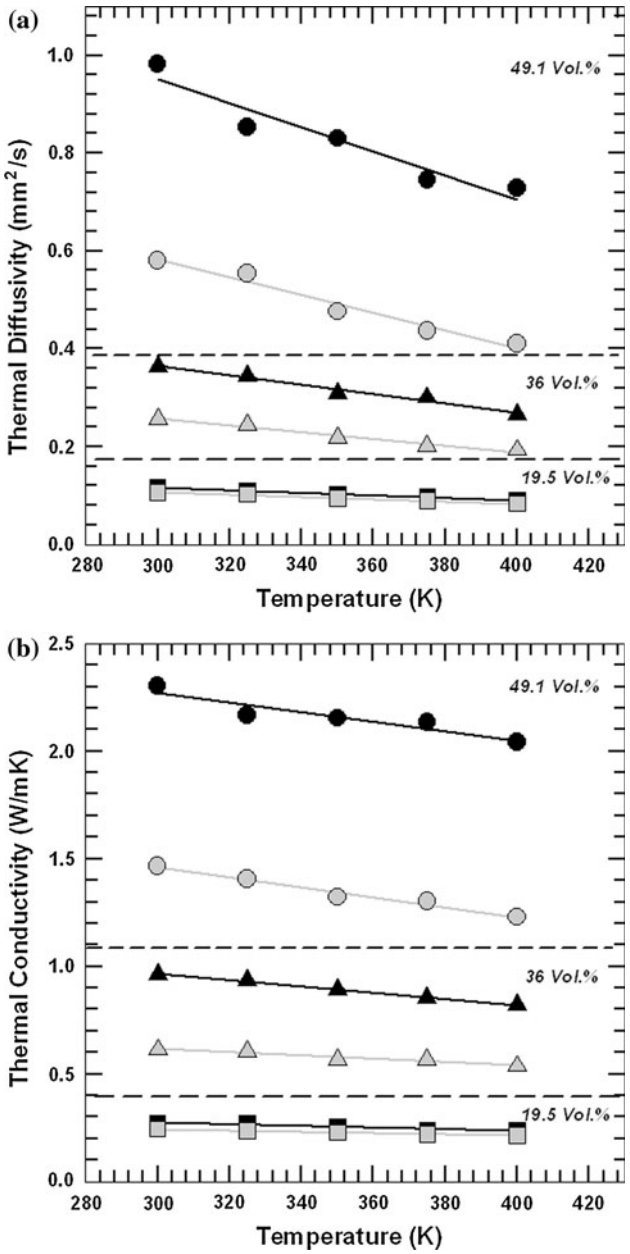

Fig. 11 Thermal conductive properties of composites as a function of operating temperature: **a** thermal diffusivity and **b** thermal conductivity. The *black symbols* represent P-ETDS/Al_2O_3 and the *gray symbols* represent ETDS/Al_2O_3

The effects of temperature on the thermal properties were investigated for various electrical heat-dissipating applications, and the results are shown in Fig. 11. Similar to all dielectric materials, the thermal diffusivity and conductivity decreased with an increase in the temperature. The decrease of thermal conductivity with temperature is believed to be due to the fact that, in the devitrification process, the composites were subjected to some composition changes. This is because of the fact that with increase in test temperature the phonon vibration frequency will be quickened to make the collision possibility increase while the mean free path decreases rapidly leading to the rapid increase of its thermal resistance. From a scientific and practical point of view, the mean free path decreases and thus the contributions to the corresponding thermal resistance increase linearly with the rise of temperature, resulting in the decrease of thermal conductivity in this temperature range [47].

As expected, all composites containing PMDMS:Al_2O_3 showed more enhanced thermal conduction properties at fixed filler contents than did those without. This is due to more enhanced surface interaction strength between the filler and matrix, regardless of the electrical operating temperature.

Conclusions

Aluminum oxide containing modified polysiloxane (PMDMS:Al_2O_3) was synthesized and blended with ETDS. ETDS was formed with the pre-cured, amino-terminated oligomer at low reaction temperatures, and these oligomers blended with aluminum oxide coordinated PMDMS. The dimethylsiloxane blocks in both materials could establish the miscible phase due to their structural similarity. Other blocks in the PMDMS containing aluminum oxide provided enhanced interfacial interaction strength between the polymer matrix and fillers. As a result, the PMDMS:Al_2O_3 containing composites (P-ETDS/Al_2O_3) revealed more enhanced thermal conduction properties because of strengthened interfacial bonding at a fixed filler concentration. The conductive behaviors as a function of the filler concentration were correlated with various Agari's model. Based on the coefficient value obtained from Agari's model, PMDMS:Al_2O_3 affected the formation of the conducting path in the composite.

The effects of temperature on the thermal properties were investigated, and the results revealed that the thermal diffusivity and conductivity decreased with an increase in the temperature. In addition, all composites containing PMDMS:Al_2O_3 showed enhanced thermal conduction properties, regardless of the measuring temperature.

Acknowledgements This study (Grant No. 000440680110) was supported by Business for Cooperative R&D between Industry, Academy, and Research Institute funded Korea Small and Medium Business Administration in 2010.

References

1. Yu A, Ramesh P, Itkis ME, Bekyarova E, Haddon RC (2007) J Phys Chem C 111:7565
2. Lin W, Moon KS, Wong CP (2009) Adv Mater 21:2421

3. Mamunya Y, Boundenne A, Lebovka N, Candau Y, Lisunova M (2008) Compos Sci Technol 68:1981
4. Sim LC, Ramanan SR, Ismail H, Seetharamu KN, Goh TJ (2005) Thermochim Acta 430:155
5. Xu Y, Luo X, Chung DDL (2002) J Electron Packag 124:188
6. Wolff EG, Shneider DA (1998) Int J Heat Mass Transf 41:3469
7. Yung KC, Wang J, Yue TM (2008) J Compos Mater 42:2615
8. Lee GW, Park M, Kim J, Lee JI, Yoon HG (2006) Compos Part A Appl Sci Manuf 37:727
9. Shi Z, Radwan M, Kirihara S, Miyamoto Y, Jin Z (2009) Appl Phys Lett 95:224104
10. Li TL, Hsu SLC (2010) J Phys Chem B 114:6825
11. Zhi C, Bando Y, Terao T, Tang C, Kuwahara H, Golberg D (2009) Adv Funct Mat 19:1857
12. Yang F, Zhao X, Xiao P (2010) J Eur Ceram Soc 30:3111
13. Lee B, Dai G (2009) J Mater Sci 44:4848. doi:10.1007/s10853-009-3739-6
14. Lee ES, Lee SM, Shanefield DJ, Cannon WR (2008) J Am Ceram Soc 91:1169
15. Watari K, Ishizaki K, Tsuchiya F (1993) J Mater Sci 28:3709. doi:10.1007/BF00353168
16. Hirano M, Yamauchi N (1993) J Mater Sci 28:5737. doi:10.1007/BF00365175
17. Zhou W (2011) J Mater Sci 46:3883. doi:10.1007/s10853-011-5309-y
18. Guthy C, Du F, Brand S, Winey KI, Fischer JE (2007) J Heat Transf 129:1096
19. Biercuk MJ, Llaguno MC, Radosavljevic M, Hyun JK, Johnson AT, Fischer JE (2002) Appl Phys Lett 80:2767
20. Liu CH, Huang H, Wu Y, Fan SS (2004) Appl Phys Lett 84:4248
21. Bryning MB, Milkie DE, Islam MF, Kikkawa JM, Yodh AG (2005) Appl Phys Lett 87:161909
22. Yu A, Itkis ME, Bekyarova E, Haddon RC (2006) Appl Phys Lett 89:133102
23. Lee HH, Chou KS, Shih ZW (2005) Int J Adhes Adhes 25:437
24. Gwinn JP, Webb RL (2003) Microelectron J 34:215
25. Hong J, Lee J, Hong CK, Shim SE (2010) Curr Appl Phys 10:359
26. Wang Q, Gao W, Xie Z (2003) J Appl Polym Sci 89:2397
27. Zhou W, Qi S, Tu C, Zhao H (2007) J Appl Polym Sci 104:2478
28. Kim H, Kim J, Kim J (2010) Microelectron Reliab 50:258
29. Im H, Kim J (2010) Polym Compos 31:1669
30. McGrath JE, Riffle JS, Banthia AK, Yilgor L, Wilkes GL (1983) An overview of the polymerization of cyclosiloxanes, initiation and polymerization. In: ACS Symposium Series No. 212, Chapter 2, Washington
31. Kang DH, Lee BC (2004) Polymer (Korea) 28:143
32. Carson JK, Noureldin M (2009) Int Commun Heat Mass 36:458
33. Gustafsson SE, Karawacki E, Khan MN (1979) J Phys D Appl Phys 12:1411
34. Barrie JA, Munday K (1983) J Membr Sci 13:175
35. Bajaj P, Varshney SK (1981) Polymer 22:372
36. Horiuchi H, Irie S, Nose T (1991) Polymer 32:1970
37. Hashin Z, Shtrikman S (1962) J Appl Phys 33:3125
38. Sushumna I, Gupta RK, Ruckenstein E (1991) J Mater Res 6:1082
39. Meredith RE, Tobias CW (1962) Advances in electrochemistry and electrochemical engineering, vol 2. Wiley, New York
40. Brruggeman DAG (1935) Ann Phys 416:636
41. Meredith RE, Tobias CW (1961) J Electrochem Soc 108:286
42. Ramajo L, Reboredo M, Santiago D, Castro M (2008) J Compos Mater 42:2027
43. Agari Y, Uno T (1985) J Appl Polym Sci 30:2225
44. Scarisbrick RM (1973) J Phys D Appl Phys 6:2098
45. Markov AV (2008) Polym Sci Ser A 5:709
46. Agari Y, Tanaka M, Nagai S, Uno T (1987) J Appl Polym Sci 34:1429
47. Cecen V, Tavman IH, Kok M, Aydogdu Y (2009) Polym Compos 30:1229